

GRAVITY AND ZONAL FLOWS OF GIANT PLANETS:  
FROM THE EULER EQUATION TO THE THERMAL WIND EQUATION

HAO CAO, DAVID J. STEVENSON

Division of Geological and Planetary Sciences, California Institute of Technology, Pasadena, CA 91125

## ABSTRACT

Any non-spherical distribution of density inside planets and stars gives rise to a non-spherical external gravity and change of shape. If part or all of the observed zonal flows at the cloud deck of giant planets represent deep interior dynamics, then the density perturbations associated with the deep zonal flows could generate gravitational signals detectable by the planned *Juno* mission and the *Cassini* Proximal Orbits. It is currently debated whether the thermal wind equation (TWE) can be used to calculate the gravity field associated with deep zonal flows. Here we present a critical comparison between the Euler equation and the thermal wind equation. Our analysis shows that the applicability of the TWE in calculating the gravity moments depends crucially on retaining the non-sphericity of the background density and gravity. Only when the background non-sphericity of the planet is taken into account, the TWE makes accurate enough prediction (with a few tens of percent errors) for the high-degree gravity moments associated with deep zonal flows. Since the TWE is derived from the curl of the Euler equation and is a local relation, it necessarily says nothing about any density perturbations that contribute irrotational terms to the Euler equation and that has a non-local origin. However, the predicted corrections from these density contributions to the low harmonic degree gravity moments are not discernible from insignificant changes in interior models while the corrections at high harmonic degree are very small, tens of percent or less.

## 1. INTRODUCTION

The interior structures and dynamics of the solar system giant planets remain elusive after decades of observational, experimental and theoretical studies (cf. [Stevenson 1982](#); [Hubbard et al. 2002](#); [Guillot 2005](#); [Guillot and Gautier 2014](#), and reference therein). For example, whether present-day Jupiter and Saturn have well-defined cores remains an open question; the total enrichment of heavy elements inside Jupiter and Saturn are not well constrained; the structural and dynamical consequences of the likely on-going sedimentation of helium and neon inside Jupiter and Saturn have not been fully worked out (cf. [Stevenson and Salpeter 1977](#); [Fortney and Hubbard 2003](#); [Nettelmann et al. 2015](#)).

One lasting debate concerns the nature of the observed east-west zonal flows on the cloud layers of giant planets with amplitude on the order of 100 *m/s*: no consensus has been reached upon whether these zonal winds represent shallow atmospheric dynamics or deep interior dynamics (e.g. [Vasavada and Showman 2005](#); [Liu et al. 2008](#); [Jones and Kuzanyan 2009](#); [Kaspi et al. 2009](#); [Liu and Schneider 2010](#); [Gastine et al. 2013](#)). The forward fluid dynamics and magnetohydrodynamics (MHD) problem about the nature of giant planet zonal flows may be hard to settle given the complexity of the system and the extreme parameters involved. However, an observational fact about the depth of the zonal flows of Jupiter and Saturn will likely be established given the upcoming gravity and magnetic experiments to be carried out by the *Juno* mission ([Bolton 2010](#)) and the *Cassini* Proximal Orbits ([Spilker et al. 2014](#)). In this paper, we focus on the gravity field.

The physical principle of the gravitational sounding of giant planet zonal flows is not complicated: zonal flows

will induce local and non-local density perturbations, as well as global shape change of the planet, all of which will contribute to perturbations to the external non-spherical gravity field. Apart from observational issues such as data coverage, the analysis of the actual gravity measurement is complicated by the fact that the background external non-spherical gravity field caused by the background uniform rotation is not known a priori. Even if one would like to analyze the problem in real space (e.g. directly assess the gravity field  $\mathbf{g}$  rather than the gravity moments  $J_n$ ), one is still forced to analyze the truncated gravity field associated with high-degree gravity moments only (e.g.  $\Delta\mathbf{g}$  associated with  $J_n$ ,  $n \geq 12$  for Jupiter and Saturn). Since the upcoming gravity measurements at Jupiter and Saturn will not be sensitive to an infinite series of high-degree gravity moments due to the geometric decay, the accuracy of the individual high-degree gravity moments associated with zonal flows from a forward model is then an important issue.

The thermal wind equation (TWE) under the anelastic approximation can be used to calculate the gradient of local density perturbations  $\nabla\rho'$  associated with zonal flows, when the zonal flows are much slower than the background rotation. The measured differential rotation on the surface of Jupiter and Saturn are small compare to the background planetary rotation. In terms of the Rossby number  $Ro = u/\Omega_0 R_p$  ( $u$  is the velocity measured in the corotating frame,  $\Omega_0$  is the background rotation rate,  $R_p$  is the planetary radius),  $Ro$  at Jupiter is smaller than 0.01, and  $Ro$  at Saturn is smaller than 0.05. However, the applicability of TWE to further calculate the individual gravity moments for an oblate planet is not guaranteed a priori, given the non-local nature of the gravity moments. This applicability has been actively debated in the recent literature (cf. [Kaspi et al. 2010](#); [Kong et al. 2014](#); [Zhang et al. 2015](#)).

In this paper, we present a critical evaluation of the applicability of the thermal wind equation to calculate the zonal flow gravity moments. The gravity moments associated with deep zonal flows calculated from two versions of the thermal wind equation are compared to the full solution to the Euler equation obtained from a non-perturbative approach. We found that only when the non-sphericity of the background density and effective gravity is taken into account, the individual high-degree gravity moment calculated from the thermal wind equation is then a good approximation to the full solution. Our analysis thus suggests that, when analyzing the zonal flow gravity moments of Jupiter and Saturn using the thermal wind equation, the non-sphericity of the background state must be retained.

The paper is organized as following, section 2 introduces the definition and properties of gravity moments, section 3 presents a detailed comparison of the Euler equation and the thermal wind equation, section 4 presents the gravity moments of a uniformly rotating planet with polytrope of index unity calculated from the Euler equation using a non-perturbative approach, section 5 presents the gravity moments of a differentially rotating planet with polytrope of index unity calculated from the Euler equation, the thermal wind equation with spherical background state, and the thermal wind equation with non-spherical background state, section 6 presents a quantitative analysis of what the thermal wind equation misses, section 7 summarizes the results and discuss the implications for analyzing the gravity measurements of the *Juno* mission and the *Cassini* Proximal Orbits.

## 2. DEFINITION AND PROPERTIES OF THE GRAVITY MOMENTS

The axisymmetric gravity moments  $J_n$  are determined by the planetary interior density distribution through

$$J_n = -\frac{1}{Ma^n} \int_{\mathbf{R}^3} \rho(\mathbf{r}) r^n P_n(\cos\theta) d^3\mathbf{r}, \quad (1)$$

in which  $M$  is the mass of the planet,  $a$  is a reference radius usually chosen to be the measured equatorial radius of the planet,  $r$  is the spherical-radial distance to the center of mass of the planet,  $P_n$  is the Legendre polynomials of degree  $n$ ,  $\theta$  is the co-latitude measured from the spin-axis and the integration is over the entire volume of the planet.

It should be immediately realized that 1) if the density distribution is spherically symmetric,  $\partial\rho/\partial\theta = 0$ , all  $J_n$  with  $n \geq 1$  would be zero; 2) if the density distribution is equatorially symmetric,  $\rho(r, \theta) = \rho(r, \pi - \theta)$ , all odd-degree  $J_n$  would be zero.

If mass, equatorial radius, rotation rate and the gravity moments are the only measurements we have about a planetary body, the interpretation of gravity moments depend on extra assumptions and forward modeling of the density distributions inside the planet. The appropriate forward model for the density distribution inside a fluid planet is nothing but the appropriate governing equations of fluid dynamics. In the inviscid limit, this set of governing equation is the Euler equation. Even though the dynamics being considered are usually simple (e.g. uniform rotation or differential rotation only), the Euler equations for this particular application are

not easy to solve due to the fact that we are dealing with self-gravity. The problem is non-local: gravity at any local position depends on the density distribution over the entire planet. Mathematically, one needs to deal with integro-differential equations in general. The problem is further complicated by the fact that the equation of state (EOS) of the materials under planetary conditions are imperfectly known.

## 3. FROM THE EULER EQUATION TO THE THERMAL WIND EQUATION

### 3.1. The Euler Equation

The structure and dynamics of a self-gravitating fluid body in steady-state must be in force-balance. This force-balance in the inviscid limit is described by the steady-state Euler equation. In an inertia frame, the Euler equation reads

$$(\mathbf{u} \cdot \nabla)\mathbf{u} = -\frac{\nabla P}{\rho} - \nabla V_g, \quad (2)$$

in which  $\mathbf{u}$  is the velocity in the inertial frame,  $P$  is the pressure,  $\rho$  is the density, and  $V_g$  is the gravitational potential. The gravitational acceleration is the negative gradient of the gravitational potential:

$$\mathbf{g} = -\nabla V_g. \quad (3)$$

Considering self-gravity only, the gravitational potential is determined by the global density distribution

$$V_g(\mathbf{r}) = -\int_{\mathbf{R}^3} \frac{G}{|\mathbf{r} - \mathbf{r}'|} \rho(\mathbf{r}') d^3\mathbf{r}', \quad (4)$$

in which  $G$  is the gravitational constant, and the integration is over the entire domain of the planet.

Under the barotropic assumption (density depends on pressure only) and a velocity field that does not violate the barotropic assumption, the density distribution can be determined entirely from the Euler equation (2) given the total mass and the specific equation of state. If the fluid is baroclinic, an additional equation governing the evolution of temperature or entropy is needed to determine the density distribution.

### 3.2. The Euler Equation in an Inertial Frame for a Uniformly Rotating Planet

For a uniformly rotating planet, the velocity in the inertial frame reads

$$\mathbf{u}_0 = \Omega_0 s \hat{\phi} = \Omega_0 r \sin\theta \hat{\phi}, \quad (5)$$

here  $\Omega_0$  is the constant angular velocity,  $s$  is the cylindrical radial distance from the spin axis ( $s = r \sin\theta$ ).

It can be easily shown that

$$(\mathbf{u}_0 \cdot \nabla)\mathbf{u}_0 = \nabla Q_0 \quad (6)$$

in which  $Q_0$  is the familiar centrifugal potential

$$Q_0 = -\int_0^s \Omega_0^2 s' ds' = -\frac{\Omega_0^2 s^2}{2}. \quad (7)$$

The Euler equation now reads

$$\nabla P = -\rho \nabla (V_g + Q_0) = -\rho \nabla U, \quad (8)$$

where  $U$  is the effective potential defined as  $U = V_g + Q_0$ .

When coupled with a specific equation of state (EOS), the solution of the above Euler equation yield the shape and internal density distribution of a uniformly rotating planet. It is appropriate to denote the properties satisfying equation (8) as the background properties with a subscript 0, so equation (8) now reads

$$\nabla P_0 = -\rho_0 \nabla(V_{g_0} + Q_0) = -\rho_0 \nabla U_0. \quad (9)$$

Regardless of whether we are dealing with a barotropic fluid or not, the iso-surface of the background density always coincide with the iso-surface of the background effective potential since  $\nabla \rho_0 \times \nabla(V_{g_0} + Q_0) = 0$ .

### 3.3. The Euler Equation for a Planet with Differential Rotation and the Thermal Wind Equation

Now consider a planet with differential rotation, the velocity in the inertial frame reads

$$\mathbf{u}_1 = [\Omega_0 + \Omega'(s, z)]s\hat{\phi} = \Omega_1 s\hat{\phi}, \quad (10)$$

here  $\Omega'$  is the angular velocity of the differential rotation,  $\Omega_1$  is the total angular velocity measured in the inertial frame, while

$$\mathbf{u}' = \mathbf{u}_1 - \mathbf{u}_0 = \Omega'(s, z)s\hat{\phi} \quad (11)$$

is the zonal velocity measured in the non-inertial frame rotating at angular velocity  $\Omega_0$ .

If the angular velocity of the differential rotation depends only on the cylindrical radius ( $\partial\Omega'/\partial z = 0$ ), it can be shown that

$$(\mathbf{u}_1 \cdot \nabla)\mathbf{u}_1 = \nabla Q, \quad (12)$$

here  $Q$  is the generalized centrifugal potential

$$Q = -\int_0^s \Omega_1^2 s' ds' = -\int_0^s [\Omega_0 + \Omega'(s')]^2 s' ds'. \quad (13)$$

For an arbitrary flow, it can be shown that,

$$(\mathbf{u}_1 \cdot \nabla)\mathbf{u}_1 = \nabla Q_0 + 2\Omega_0 \hat{z} \times \mathbf{u}' + (\mathbf{u}' \cdot \nabla)\mathbf{u}', \quad (14)$$

it should be recognized that  $-\nabla Q_0$  and  $-2\Omega_0 \hat{z} \times \mathbf{u}'$  are simply the centrifugal acceleration and the Coriolis acceleration in the rotating frame with angular velocity  $\Omega_0$ .

Substitute equation (14) and equation (9) into the Euler equation (2), and write the density and Pressure as the sum of the background and the perturbation

$$\rho_1 = \rho_0 + \rho' \quad (15)$$

$$P_1 = P_0 + P', \quad (16)$$

we get

$$2\rho_0 \Omega_0 \hat{z} \times \mathbf{u}' + \rho_0 (\mathbf{u}' \cdot \nabla)\mathbf{u}' + \rho_0 \nabla V_{g'} = \quad (17a)$$

$$-\rho' \nabla V_{g_0} - \rho' \nabla Q_0 - \nabla P' \quad (17b)$$

$$-2\rho' \Omega_0 \hat{z} \times \mathbf{u}' - \rho' (\mathbf{u}' \cdot \nabla)\mathbf{u}' - \rho' \nabla V_{g'}, \quad (17c)$$

where  $V_{g'}$  is the gravitational potential of the density perturbations  $\rho'$

$$V_{g'}(\mathbf{r}) = -\int_{\mathbf{R}^3} \frac{G}{|\mathbf{r} - \mathbf{r}'|} \rho'(\mathbf{r}') d^3 r'. \quad (18)$$

An order of magnitude analysis yields the first estimate about the relative importance of each of the terms in equation (17). 1) The ratio between the Reynolds

stress associated with the zonal flows  $\rho_0(\mathbf{u}' \cdot \nabla)\mathbf{u}'$  and the Coriolis term  $2\rho_0 \Omega_0 \hat{z} \times \mathbf{u}'$  is on the order of the Rossby number:  $\sim 1\%$  for Jupiter and  $\sim 5\%$  for Saturn. 2) The gravity anomaly associated with the density perturbation,  $\nabla V_{g'}$ , is smaller than the background gravity by a factor of  $\rho'/\rho_0$ . Zhang et al. (2015) pointed out that  $\rho_0 \nabla V_{g'}$  could be comparable to  $\rho' \nabla V_{g_0}$ . 3) The gradient of the pressure perturbation  $\nabla P'$  is likely comparable to  $\rho' \nabla U_0$ . This can be shown easily for a polytropic equation of state  $P = K\rho^{(1+1/n)}$ . The perturbative pressure can now be expressed as a function of the density

$$P' = P - P_0 \quad (19a)$$

$$= K(\rho_0 + \rho')^{(1+1/n)} - K\rho_0^{(1+1/n)}. \quad (19b)$$

Assuming  $\rho'/\rho_0 \ll 1$ , one can Taylor expand the above equation. Retaining the first order term only, we get

$$P' = (1 + \frac{1}{n})K\rho_0^{1/n} \rho'. \quad (20)$$

Taking the gradient of  $P'$ , and make use of the hydrostatic balance of the background state, we get

$$\nabla P' = -\frac{1}{n}\rho' \nabla U_0 + (1 + \frac{1}{n})K\rho_0^{1/n} \nabla \rho'. \quad (21)$$

(Note, the second term in (21) can be comparable to the first term  $\frac{1}{n}\rho' \nabla U_0$  given the likely small characteristic scale of  $\rho'$ .) And 4) the ratio of each of the last three terms in equation (17) to its corresponding LHS term is  $|\rho'/\rho_0|$ . One cautionary note about the value of  $|\rho'/\rho_0|$ . As we will see, although it is true that  $|\rho'/\rho_0|$  is smaller than one in the bulk interior of the planet, this is not true for regions very near the surface.

Taking the curl of the equation (17), retaining only the first term on the left hand side (LHS) and the first two terms on the right hand side (RHS), and making use of the mass continuity equation under the anelastic approximation, we arrive at the generic thermal wind equation (TWE)

$$(2\Omega_0 \cdot \nabla)(\rho_0 \mathbf{u}) = -\nabla \rho' \times \mathbf{g}_{\text{eff}}, \quad (22)$$

where the background effective gravity  $\mathbf{g}_{\text{eff}}$  is

$$\mathbf{g}_{\text{eff}} = -\nabla U_0 = -\nabla(V_{g_0} + Q_0). \quad (23)$$

Note, first, that since the curl has been taken, information has been lost. Specifically, there are solutions to the curl free part of equation which can contribute to density perturbations. In addition, there will be density perturbations with non-local origin because of 1) the gravity resulting from the local density anomalies that are required by the TWE and 2) the global shape change associated with the net angular moment of the zonal flows. The non-local density perturbations associated with the gravity anomaly resulting from the local density perturbations required by the TWE was recognized by Zhang et al. (2015). However, as we will show in section 6, this type of non-local density perturbations are far smaller than the non-local density perturbations associated with the global shape change. More importantly, the total non-local density perturbations do not contribute much to the high-degree gravity moments.

One further simplification to the generic thermal wind equation (22) usually adopted in estimating the zonal

flow gravity field is to assume that the background effective gravity is spherically symmetric (e.g. [Kaspi et al. 2010](#); [Liu et al. 2013](#)). One argument for this simplification is the uniqueness of  $J_n$  calculated under this assumption despite a non-uniqueness in the density perturbations calculated from the TWE. However, we will show that the mathematical uniqueness gained from this assumption does not worth the physical relevance being sacrificed. And the mathematical non-uniqueness in the density perturbations from the TWE can be treated through physically reasonable assumptions.

#### 4. GRAVITY MOMENTS OF A UNIFORMLY ROTATING PLANET WITH POLYTROPE OF INDEX UNITY

To compare the density perturbations and gravity moments associated with the deep zonal flows calculated from the thermal wind equation to the full solution of the Euler equation, we first solve the Euler equation for a uniformly rotating planet. Here, we adopt a polytropic equation of state

$$P = K\rho^{(1+1/n)}, \quad (24)$$

in which  $K$  is a constant, and the polytropic index  $n$  is set to 1. A polytrope of index unity not only is a reasonable approximation to the adiabatic equation of state under Jupiter conditions but also makes the Euler equation easier to deal with since  $\nabla P/\rho$  now reduces to  $2K\nabla\rho$ . The divergence of the Euler equation (9) yields

$$\nabla^2\rho_0 + \frac{2\pi G}{K}\rho_0 = \nabla^2\left(\frac{\Omega_0^2 s^2}{4K}\right), \quad (25)$$

which governs the background density distribution subject to the boundary condition that the outer boundary defined by  $\rho_0(r, \theta) = 0$  is also an equal-potential surface

$$U_0(\rho_0(r, \theta) = 0) = \text{const}. \quad (26)$$

The general solution to the above equation takes the form

$$\rho = \rho_P + \sum_{n=0}^{n_{max}} A_n j_n(kr) P_n(\cos\theta), \quad (27)$$

where  $\rho_P = \Omega_0^2/2\pi G$ ,  $j_n$  is the spherical Bessel function of the first kind of degree  $n$ ,  $k = \sqrt{2\pi G/K}$ , and  $P_n$  is the Legendre polynomials of degree  $n$ , and  $A_n$  are the coefficients to be determined by the boundary conditions as well as the total mass.

The existence of the analytical form of the general solution enables a non-perturbative approach to this problem (e.g. [Wisdom 1996](#) unpublished; [Hubbard 1999](#)). Under this circumstance, there is no need to define the level surfaces and solve for the figure equations explicitly. Here we point out a few key aspects of this non-perturbative approach: 1) the coefficients  $A_n$  are the only variables need to be solved explicitly, both the outer boundary shape, which defines the solution domain, and the internal density distribution are uniquely determined by  $A_n$ ; 2) the outer boundary is not constrained to be an exact ellipsoid of revolution, and the resulted outer boundary indeed differs from an exact ellipsoid of revolution; 3) the traditional geophysical expansion of the external gravitational potential  $U_0$  is used to calculate the potential at the outer boundary, since its convergence under Jupiter

**Table 1**  
Comparison Between the Polytrope Model and Jupiter.

	Jupiter	Polytrope Model <sup>a</sup>
Mass [kg]	$1.8983 \times 10^{27}$	$1.8983 \times 10^{27}$
Rotation Period [hrs]	9.925	9.925
Equatorial Radius [km]	71492	71419.8
Polar Radius [km]	66854	66876.0
$q = \frac{\Omega_0^2 a^3}{GM}$	0.08919...	0.08892...
$J_2 \times 10^{-6}$	14696.43	13949.81
$J_4 \times 10^{-6}$	-587.14	-528.88
$J_6 \times 10^{-6}$	34.25	29.87

<sup>a</sup> $P = K\rho^2$  with  $K = 2 \times 10^5 [m^5 kg^{-1} s^{-2}]$

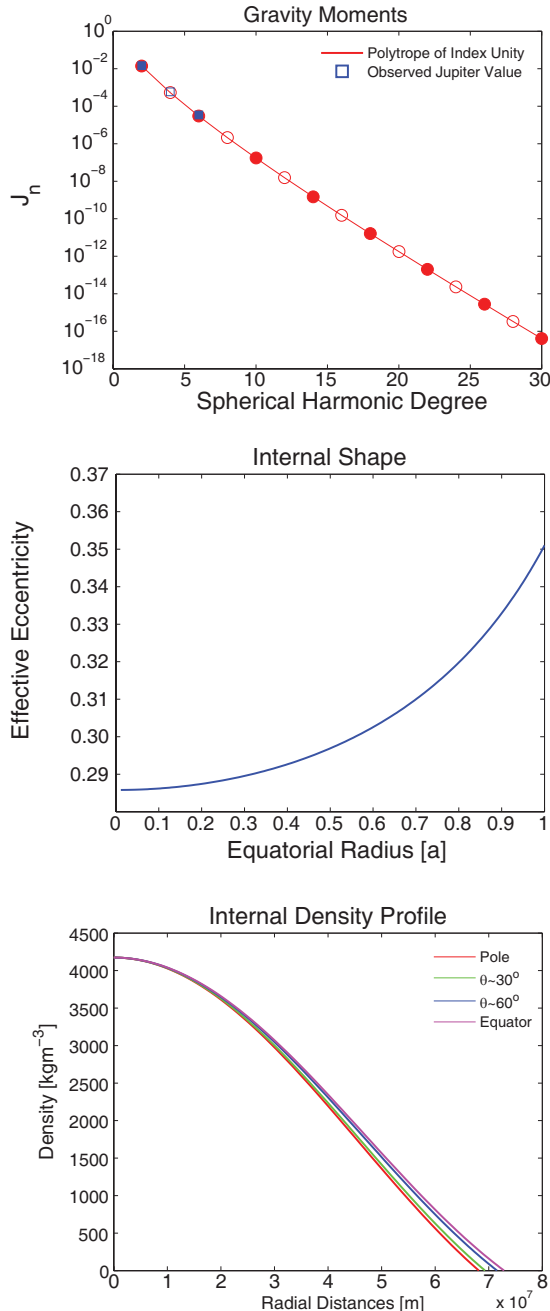
and Saturn like surface distortions has been shown by [Hubbard et al. \(2014\)](#).

Fig. 1 shows the gravity moments, the internal shape, and the internal density distribution from one of our calculations with  $K = 2 \times 10^5 [m^5 kg^{-1} s^{-2}]$ . The total mass and the background rotation rate have been fixed to the measured values of Jupiter. Comparison of the equatorial radius, the polar radius, the smallness parameter  $q$ , and the first few gravity moments between the model and observed values of Jupiter is listed in Tab. 1. It can be seen that the first three gravity moments of this model planet are reasonably close to those measured at Jupiter. The effective eccentricity of the shape of the planet decreases from  $\sim 0.35$  near the surface of the planet to  $\sim 0.29$  near the center of the planet. And the shape change occurs mostly in the outer part of the planet. The effective eccentricity is defined as  $ec(r) = \sqrt{1 - r_b^2/r_a^2}$ , where  $r_a$  and  $r_b$  are the equatorial radius and the polar radius of a level surface. The reason we call this effective eccentricity lies in our finding that the level surface are not exact ellipsoid of revolutions. Fig. 2 shows the deviation of the outer boundary surface shape from an exact ellipsoid of revolution with the equatorial radius and polar radius fixed to the corresponding values of the outer surface. The deviation is dominant by  $\sin^2 2\theta$  with an amplitude  $\sim 5 \times 10^{-4}$ , and thus corresponds to the second order correction in the standard expansion of level surface in terms of the effective eccentricity (e.g. equation 30.3 in [Zharkov and Trubitsyn 1978](#)). We noticed that some published solutions of this problem are based on the assumption that the outer boundary shape is an exact ellipsoid of revolution (e.g. [Kong et al. 2013, 2015](#)).

#### 5. GRAVITY MOMENTS OF A DIFFERENTIALLY ROTATING PLANET WITH POLYTROPE OF INDEX UNITY

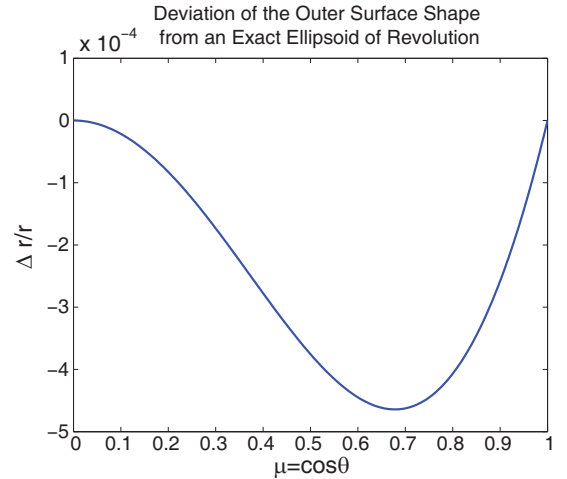
We now turn to a planet with differential rotation. The total mass, background rotation rate, and the equation of the state is taken to be the same as those in the study of a uniformly rotating planet. The differential rotation is chosen to have angular velocity as a function of cylindrical-radial distance only ( $\partial\Omega/\partial z = 0$ ). This consideration is mainly motivated by the fact that such velocity profile does not violate the barotropic assumption, and a full solution to the Euler equation can be obtained without further complications. (Of course, there is no reason to suppose that the planets obey this precisely.) The full solution of the Euler equation can then be compared to those obtained from the thermal wind equation.

Fig. 3 shows the specific zonal wind profile adopted



**Figure 1.** Gravity moments  $J_n$ , internal shape measured by the effective eccentricity  $ec = \sqrt{1 - r_b^2/r_a^2}$ , and internal density distribution of a uniformly rotating planet with the same mass and rotation rate as Jupiter but with a polytropic equation of state of index unity with  $K = 2 \times 10^5 [m^5 kg^{-1} s^{-2}]$ . All these quantities are calculated from the Euler equation using a non-perturbative approach based on the general solution equation (27). For  $J_n$ , filled (open) symbols represent positive (negative) values.

in this study. This specific zonal wind profile is a damped version of the observed zonal flow on the surface of Jupiter: the strong super-rotation right at the equator and the sub-rotation next to it follow closely those observed on the northern hemisphere Jupiter, while the rest of the zonal flows are much weaker compared to those measured on the surface of Jupiter, and there effectively is no zonal flow inside  $0.80 R_J$ . The wind is weaker than  $2.5 m/s$  inside  $0.90 R_J$ , and is weaker than  $1 mm/s$  inside



**Figure 2.** Deviation of the outer surface shape from that of an exact ellipsoid of revolution with the equatorial radius and the polar radius fixed to the corresponding values of the outer surface. The deviation shows a dominant component of  $\sin^2 2\theta$  with amplitude  $\sim 5 \times 10^{-4}$ . This corresponds to the second order correction in the standard expansion of level surface in terms of the effective eccentricity (e.g. equation 30.3 in Zharkov and Trubitsyn 1978).

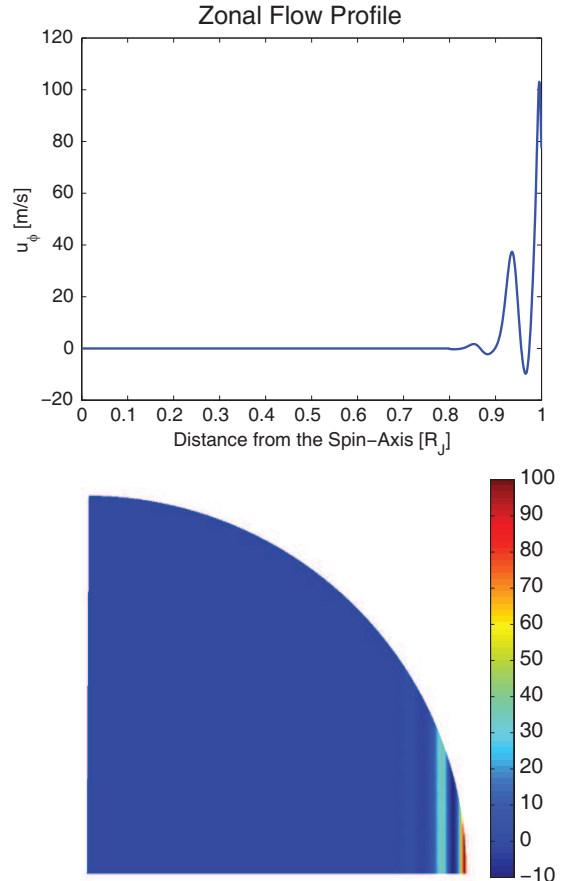


**Figure 3.** The specific zonal wind profile considered in this study. This wind profile is a damped version of the surface wind profile observed on the northern hemisphere of Jupiter, and these winds are assumed to be constant along the direction parallel to the spin-axis.

$0.80 R_J$ . The density perturbations and gravity moments associated with this wind profile are then calculated using three different approaches: the Euler equation, the

thermal wind equation with spherical background state, and the thermal wind equation with non-spherical background state.

### 5.1. Euler Equation Solution

With differential rotation on cylinders and a polytrope of index unity, the divergence of the Euler equation (2) now reads

$$\nabla^2 \rho + \frac{2\pi G}{K} \rho = -\nabla^2 \left( \frac{Q}{2K} \right), \quad (28)$$

where  $Q$  is the generalized centrifugal potential (13). The solution to this equation takes the same functional form as (27). The difference is that the specific solution  $\rho_P$  is now a function of cylindrical radius  $s$  rather than a constant. The specific solution  $\rho_P(s)$  for the wind profile we are considering can be obtained via numerically integrating equation (28) with the inner boundary condition  $\rho_P(0) = \Omega_0^2/2\pi G$ . We can solve for the internal density distribution and gravity moments  $J_n$  associated with the differential rotation using the same non-perturbative approach.

The upper panel of Fig. 4 compares the the gravity moments associated with the zonal flows shown in Fig. 3 to the gravity moments associated with the background uniform rotation  $J_n$ . It should be emphasized here that we are solving the full Euler equation to get the total gravity moments for the case with zonal flows, rather than solving for the perturbations  $\Delta J_n$  only. One aspect of the full solution is that the outer boundary shape of the planet gets further changed when zonal winds are included. It can be seen from the upper panel of Fig. 4 that the gravity moments associated with the zonal flows shown in Fig. 3 exceeds those from the background rotation by more than 100% starting from degree 12. Tab. 2 lists the values of the gravity moments  $\Delta J_n$  associated with the zonal flows shown in Fig. 3 calculated from three different approaches.

We now proceed to solve for the gravity moments and density perturbations associated with the same zonal flows using the thermal wind equation.

### 5.2. Thermal Wind Equation with Spherical Background Density and Gravity

We first consider the thermal wind equation under the simplification that reduces both the background density and the background effective gravity to a spherically symmetric state. This is the simplification adopted in almost all published calculations of the zonal flow gravity using the thermal wind equation (e.g. Kaspi et al. 2010; Liu et al. 2013). This simplification is equivalent to assume the background rotation rate is zero. The thermal wind equation now reads

$$2|\Omega_0| \frac{\partial[\rho_0(r)\mathbf{u}']}{\partial z} = -\frac{1}{r} \frac{\partial \rho'}{\partial \theta} \mathbf{e}_\theta \times (-|g_0(r)|\mathbf{e}_r). \quad (29)$$

The spherically symmetric background density and background effective gravity corresponding to a planet with the same mass and the same polytropic equation of state can be obtained analytically or through averaging the background solution obtained from the Euler equation.

The gravity moments associated with the zonal flows shown in Fig. 3 calculated from the thermal wind equation with spherically symmetric background density and

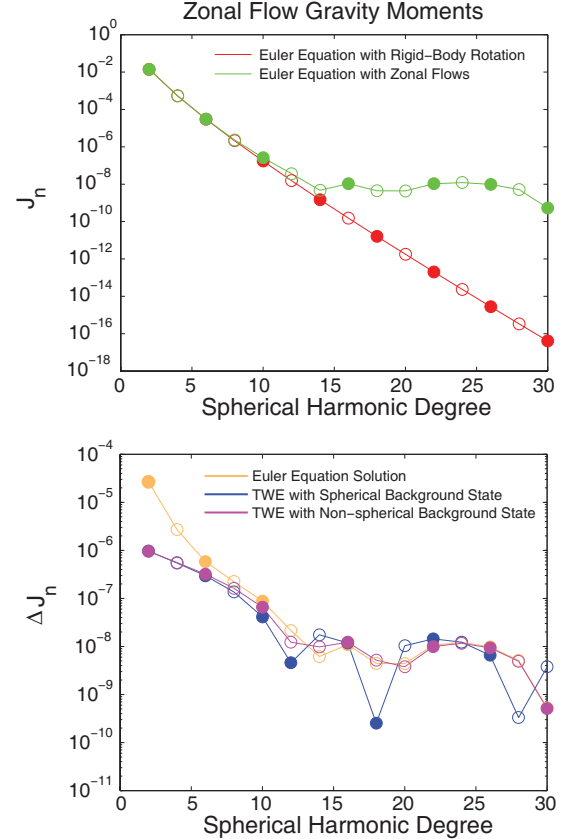


**Figure 4.** Gravity moments associated with deep equatorial zonal flows calculated from the Euler equation compared to the background gravity moments (upper panel) and those calculated from the thermal wind equation (lower panel). For the comparison with the TWE solutions (lower panel), only  $\Delta J_n$  are shown. For  $J_n$  and  $\Delta J_n$ , filled (open) circles represent positive (negative) values.

**Table 2**  
Zonal wind induced  $\Delta J_n$  calculated from different methods.

	Euler Equation	Spherical TWE <sup>a</sup>	Non-spherical TWE <sup>b</sup>
$\Delta J_2$	$2.66 \times 10^{-5}$	$9.40 \times 10^{-7}$	$9.49 \times 10^{-7}$
$\Delta J_4$	$-2.70 \times 10^{-6}$	$-5.08 \times 10^{-7}$	$-5.53 \times 10^{-7}$
$\vdots$	$\vdots$	$\vdots$	$\vdots$
$\Delta J_{12}$	$-2.14 \times 10^{-8}$	$3.77 \times 10^{-9}$	$-1.24 \times 10^{-8}$
$\Delta J_{14}$	$-6.19 \times 10^{-9}$	$-1.29 \times 10^{-8}$	$-9.28 \times 10^{-9}$
$\Delta J_{16}$	$1.08 \times 10^{-8}$	$8.24 \times 10^{-8}$	$1.19 \times 10^{-8}$

<sup>a</sup>Thermal wind equation with spherical background density and spherical background gravity.

<sup>b</sup>Thermal wind equation with non-spherical background density and non-spherical background gravity.

spherically symmetric background gravity is compared to those calculated from the Euler equation in Fig. 4 and in Tab. 2. Only  $\Delta J_n$  are shown in the lower panel of Fig. 4. It can be seen that some of the individual high-degree gravity moments calculated from this simplified thermal wind equation can be wrong by more than 100% (e.g.  $\Delta J_{12}$ ,  $\Delta J_{14}$ ) and can take the wrong sign (e.g.  $\Delta J_{12}$ ).

### 5.3. Thermal Wind Equation with Non-spherical Background Density and Effective Gravity

We now proceed to calculate the density perturbation and gravity moments associated with zonal flows using

the generic thermal wind equation with non-spherical background density distribution and non-spherical background effective gravity

$$(2\Omega_0 \cdot \nabla)(\rho_0 \mathbf{U}) = -\nabla \rho' \times \mathbf{g}_{\text{eff}}. \quad (30)$$

For a polytrope of index of unity, the background effective gravity  $\mathbf{g}_{\text{eff}}$  is simply

$$\mathbf{g}_{\text{eff}} = -\nabla U_0 = \frac{\nabla P_0}{\rho_0} = 2K \nabla \rho_0, \quad (31)$$

which can be easily calculated since  $\nabla \rho_0$  are entirely determined by the coefficients  $A_n$ .

With non-spherical effective gravity, the TWE now yields the gradient of the density perturbations  $\nabla \rho'$  along the tangent of equal-potential surfaces in the meridional plane instead of the gradient of the density perturbations along the  $\theta$  direction. To get the density perturbations  $\rho'(r, \theta)$  with non-spherical effective gravity, one would simply integrate  $\nabla \rho'$  along the tangent of equal-potential surfaces in the meridional plane

$$\rho'(\xi, l) = \int_{l'=0}^{l'=l} \nabla \rho' \cdot d\mathbf{l}' + \rho'_c(\xi), \quad (32)$$

here  $\xi$  is measured along the direction perpendicular to the equal-potential surface,  $l$  and  $dl'$  are the meridional arc length measured on the equal-potential surface, and  $\rho'_c(\xi)$  is a “constant of integration” which is only a function of  $\xi$ . Since  $\nabla \rho'_c(\xi) \times \mathbf{g}_{\text{eff}} = 0$ , this “constant of integration” has zero contribution to the generic thermal wind equation. It is clear then that TWE itself cannot supply the “constant of integration”. However, the only meaningful choice in this situation is  $\rho'_c(\xi) = 0$  since there is no permitted function of  $\xi$  alone (including a constant offset of density everywhere) that can be added to the background density field and preserves the solution to hydrostatic equilibrium.

It can be seen from Fig. 4 and Tab. 2 that for  $n \geq 12$ ,  $\Delta J_n$  associated with zonal flows calculated from thermal wind equation with non-spherical background state is much closer to the full solution than those calculated from the thermal wind equation with spherical background state. All  $\Delta J_n$  now take the correct sign, and the amplitude difference is now within 50% for individual  $\Delta J_n$ .

#### 6. WHAT THE THERMAL WIND EQUATION MISSES: GLOBAL SHAPE CHANGE, NON-LOCAL AND IRRATIONAL DENSITY CONTRIBUTIONS

As discussed in section 3.3, density perturbations that contribute irrotationally to the Euler equation and that have a non-local origin must necessarily exist. It can be seen from Fig. 4b and Tab. 2 that the low degree gravity moments associated with zonal flows ( $\Delta J_2$ ,  $\Delta J_4$ ) estimated from either version of the thermal wind equation are a factor of 25 and a factor of 5 smaller than those calculated from the full Euler equation. These relatively large discrepancies for low-degree gravity moments arises from the fact that the planet responds to the zonal flows in a non-local manner, and irrotational density perturbations are not negligible.

Fig. 5 compares the density perturbations associated with deep zonal flows (shown in Fig. 3) calculated from the Euler equation and the thermal wind equation. The

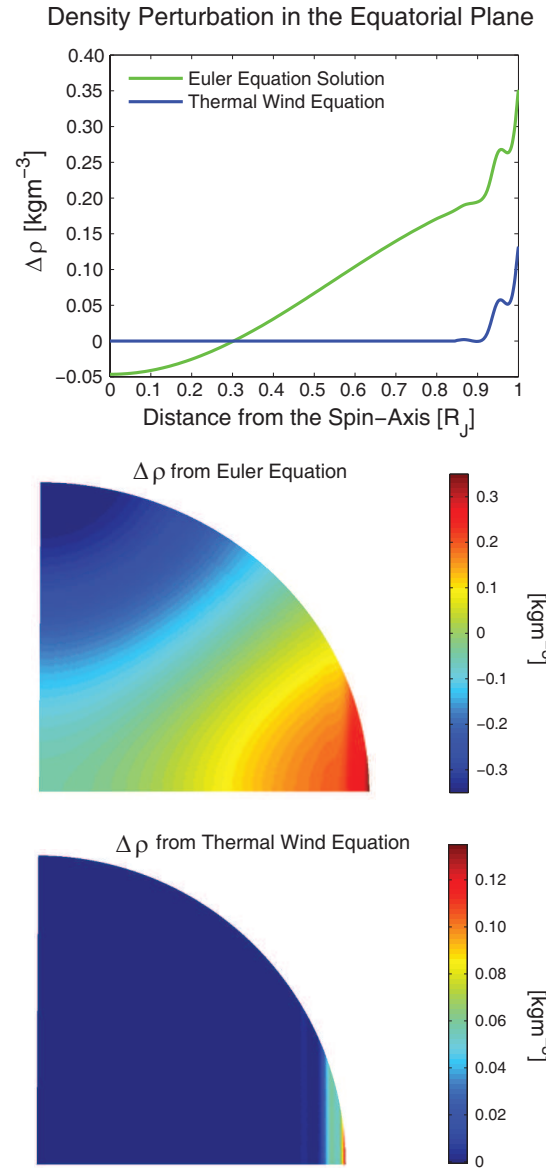


**Figure 5.** Density perturbations associated with deep zonal flows (shown in Fig. 3) calculated from the Euler equation and the thermal wind equation. It can be seen that the thermal wind equation captures the local small-scale density perturbations but misses the non-local large-scale density perturbations.

density perturbations calculated from two version of the thermal equation are both localized and are visually similar, thus only the density perturbations calculated from the thermal wind equation with spherical background state is shown for clarity. It can be seen from Fig. 5 that the thermal wind equation captures the local small-scale density perturbations directly associated with the local small-scale zonal flows but misses the large-scale density perturbations (with a dominant degree-2 structure) associated with the global shape change of the planet related to the net angular moment of the zonal flows. The specific zonal wind profile we are considering have a net positive total angular moment, as a result the planet shrinks in the polar direction while expands in the equatorial direction.

Fig. 6 shows the outer boundary shape change of the entire planet caused by the localized zonal flows shown in

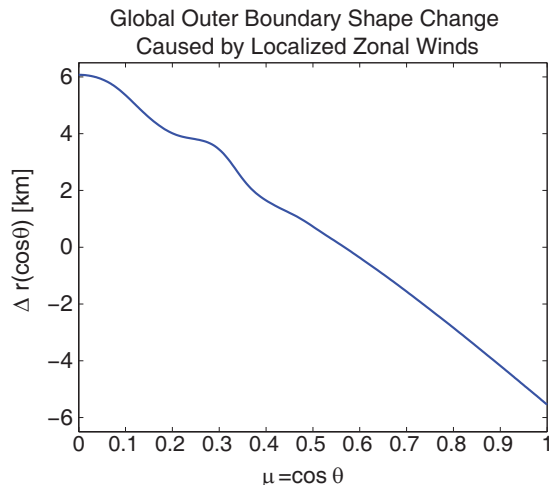


**Figure 6.** Global outer boundary shape change induced by the localized deep zonal flow shown in Fig. 3. It can be seen that the localized equatorial jet of Jupiter can induce a change of the outer boundary position by  $\pm 6km$ .

Fig. 3. It can be seen that the equatorial radius increased by  $\sim 6 km$ , while the polar radius decreased by  $\sim 6 km$ . Small-scale shape changes spatially correlated with the local zonal flows are also evident Fig. 6. This shape change by  $\sim 6 km$  can indeed account for most of the large-scale density perturbations. The radial gradient of the background density near the surface of the model planet is around  $6 \times 10^{-5} kg/m^4$ . A  $6 km$  change would thus introduce a density perturbation on the order of  $0.36 kg/m^3$ , very close to what the full solution yields.

Zhang et al. (2015) proposed a gravitational correction to the thermal wind equation by including the gravitational anomalies from the local density perturbation required by the TWE: the curl of the  $\rho_0 \nabla V_g$  term. However, this correction is very limited since it fails to account for the global shape change which is the dominant contributor to the density perturbations of non-local origin. We performed an independent calculation of the gravitational correction as proposed in Zhang et al. (2015), and find it can only account for a very insignificant portion of the global correction needed. For  $\Delta J_2$ , the gravitational correction can only provide a  $\sim 50\%$  correction while a  $\sim 2500\%$  correction is needed. For the high-degree moments with  $n \geq 12$ , the gravitational correction can only provide corrections less than 5%.

A cautionary note here is about the wind-induced low-degree gravity moments. There are at least two issues here: 1) the thermal wind equation (TWE), with or without the non-sphericity of the background state, cannot provide a meaningful prediction of the wind-induced low-degree gravity moments, neither can the thermal-gravitational wind equation (TGWE); 2) and more importantly, the wind induced low-degree gravity moments are insignificant corrections to the background low-degree gravity moments (e.g 0.2% correction to  $J_2$  and 0.5% to  $J_4$  for the particular wind profile considered here), and can be easily offset by uncertainties in the background state (such as uncertainties in our knowledge about the equation of state, heavy element distribution, etc.).

## 7. SUMMARY AND DISCUSSION

In this paper, we present a critical examination of the applicability of the thermal wind equation under anelastic assumption to calculate the gravity moments associated with zonal flows of giant planets. We first derive the thermal wind equation from the Euler equation and show that the thermal wind equation is a good approximation to the local dynamics when the Rossby number of the zonal flow measured in the co-rotation frame is much smaller than one. It is also pointed out that the thermal wind equation is a local treatment when the background effective gravity is used, while the full problem is non-local.

We then solve the full Euler equation under self-gravity for a planet with polytrope of index unity. A non-perturbative approach based on the general solution to the inhomogeneous Helmholtz equation is employed. We first solve for the shape, density profile, and the gravity moments of a uniformly rotating planet. It is found that the outer boundary shape has a significant deviation, on the second order, from an exact ellipsoid of revolution. The impact of the assumption that the outer boundary shape is an exact ellipsoid of revolution adopted in some studies of this problem (e.g. Kong et al. 2013, 2015) on their solutions thus requires further investigation.

For Jupiter-like zonal flows but confined to the equatorial region and assumed to be constant on cylinders (e.g. Fig. 3), the associated density perturbations and gravity moments are then calculated from three different methods: the full solution to the Euler equation, the thermal wind equation with spherical background state, and the thermal wind equation with non-spherical background state. We find that 1) starting at degree 12 the gravity moments associated with this particular wind profile exceed the gravity moments associated with the background rotation by more than 100%; 2) the individual high-degree gravity moments calculated from the thermal wind equation with spherical background density and gravity can be wrong by 100% and can take the wrong sign; 3) the individual high-degree gravity moments calculated from the thermal wind equation with non-spherical background density and effective gravity is a good approximation to the full solution to the Euler equation, the difference is within 50%; 4) for low-degree gravity moments associated with zonal flows, global shape change to the planet caused by the net angular moments of the zonal flows is the dominant contributor. This global shape change is missed in the thermal wind equation as well as in the thermal-gravitational wind equation (Zhang et al. 2015). However, the wind-induced low-degree gravity moments may not be a concern since they are most likely indiscernible from uncertainties in the background state.

A clear message from this study to the analysis of upcoming *Juno* and *Cassini* gravity measurements is that the non-spherical nature of the background density and effective gravity should be taken into account when using the thermal wind equation to forward calculate the gravity moments associated with the zonal flows.

## REFERENCES

- D. J. Stevenson, Annual Review of Earth and Planetary Sciences **10**, 257 (1982).

- W. B. Hubbard, A. Burrows, and J. I. Lunine, *ARA&A* **40**, 103 (2002).
- T. Guillot, *Annual Review of Earth and Planetary Sciences* **33**, 493 (2005), astro-ph/0502068.
- T. Guillot and D. Gautier, *ArXiv e-prints* (2014), 1405.3752.
- D. J. Stevenson and E. E. Salpeter, *ApJS* **35**, 239 (1977).
- J. J. Fortney and W. B. Hubbard, *Icarus* **164**, 228 (2003), astro-ph/0305031.
- N. Nettelmann, J. J. Fortney, K. Moore, and C. Mankovich, *MNRAS* **447**, 3422 (2015), 1412.4202.
- A. R. Vasavada and A. P. Showman, *Reports on Progress in Physics* **68**, 1935 (2005).
- J. Liu, P. M. Goldreich, and D. J. Stevenson, *Icarus* **196**, 653 (2008), 0711.3922.
- C. A. Jones and K. M. Kuzanyan, *Icarus* **204**, 227 (2009).
- Y. Kaspi, G. R. Flierl, and A. P. Showman, *Icarus* **202**, 525 (2009).
- J. Liu and T. Schneider, *Journal of Atmospheric Sciences* **67**, 3652 (2010), 0910.3682.
- T. Gastine, J. Wicht, and J. M. Aurnou, *Icarus* **225**, 156 (2013), 1211.3246.
- S. J. Bolton, in *IAU Symposium*, edited by C. Barbieri, S. Chakrabarti, M. Coradini, and M. Lazzarin (2010), vol. 269 of *IAU Symposium*, pp. 92–100.
- L. J. Spilker, N. Altobelli, and S. G. Edgington, *AGU Fall Meeting Abstracts* p. A1 (2014).
- Y. Kaspi, W. B. Hubbard, A. P. Showman, and G. R. Flierl, *Geophys. Res. Lett.* **37**, L01204 (2010).
- D. Kong, X. Liao, K. Zhang, and G. Schubert, *ApJL* **791**, L24 (2014).
- K. Zhang, D. Kong, and G. Schubert, *ApJ* **806**, 270 (2015).
- J. Liu, T. Schneider, and Y. Kaspi, *Icarus* **224**, 114 (2013).
- W. B. Hubbard, *Icarus* **137**, 357 (1999).
- W. Hubbard, G. Schubert, D. Kong, and K. Zhang, *Icarus* **242**, 138 (2014), ISSN 0019-1035.
- V. N. Zharkov and V. P. Trubitsyn, *Physics of planetary interiors* (1978).
- D. Kong, K. Zhang, G. Schubert, and J. Anderson, *ApJ* **763**, 116 (2013).
- D. Kong, K. Zhang, and G. Schubert, *MNRAS* **448**, 456 (2015).